Uniform semiclassical approximations of the nonlinear Schrödinger equation by a Painlevé mapping

2006 J. Phys. A: Math. Gen. 39 14687

(http://iopscience.iop.org/0305-4470/39/47/012)

INSTITUTE OF PHYSICS PUBLISHING JOURNAL OF PHYSICS A: MATHEMATICAL AND GENERAL

J. Phys. A: Math. Gen. **39** (2006) 14687–14697 doi:10.1088/0305-4470/39/47/012

Uniform semiclassical approximations of the nonlinear Schrödinger equation by a Painlevé mapping

D Witthaut and H J Korsch

FB Physik, Technische Universität Kaiserslautern, D-67653 Kaiserslautern, Germany

Received 6 July 2006, in final form 11 September 2006
Published 8 November 2006
Online at stacks.iop.org/JPhysA/39/14687

Abstract

A useful semiclassical method to calculate eigenfunctions of the Schrödinger equation is the mapping to a well-known ordinary differential equation, such as for example Airy's equation. In this paper, we generalize the mapping procedure to the nonlinear Schrödinger equation or Gross–Pitaevskii equation describing the macroscopic wavefunction of a Bose–Einstein condensate. The nonlinear Schrödinger equation is mapped to the second Painlevé equation (P_{II}), which is one of the best-known differential equations with a cubic nonlinearity. A quantization condition is derived from the connection formulae of these functions. Comparison with numerically exact results for a harmonic trap demonstrates the benefit of the mapping method. Finally we discuss the influence of a shallow periodic potential on bright soliton solutions by a mapping to a constant potential.

PACS numbers: 03.65.Ge, 03.65.Sq, 03.75.−b

(Some figures in this article are in colour only in the electronic version)

1. Introduction

In the case of low temperatures, the dynamics of a Bose–Einstein condensate (BEC) can be described in a mean-field approach by the nonlinear Schrödinger equation (NLSE) or Gross–Pitaevskii equation (see, e.g., [1])

$$\left(-\frac{\hbar^2}{2M}\frac{\partial^2}{\partial x^2} + V(x) + g|\psi(x,t)|^2\right)\psi(x,t) = \mathrm{i}\hbar\frac{\partial\psi(x)}{\partial t}, \tag{1}$$

where g is the nonlinear interaction strength. Stationary nonlinear eigenstates of the NLSE satisfying $\psi(x,t) = \exp(-\mathrm{i}\mu t/\hbar)\psi(x)$ fulfil the time-independent NLSE

$$\left(-\frac{\hbar^2}{2M}\frac{\mathrm{d}^2}{\mathrm{d}x^2} + V(x) + g|\psi(x)|^2\right)\psi(x) = \mu\psi(x). \tag{2}$$

These nonlinear eigenstates are of course no eigenstates in the sense of linear algebra, rather they should be interpreted as the stationary states of an infinite-dimensional dynamical system.

However these stationary states are still of fundamental importance for understanding the nonlinear dynamics of a BEC. For example, the self-trapping transition of a two-mode BEC is understood by a bifurcation of the nonlinear eigenstates [2, 3]. Generally, it has been shown that an adiabatic theorem also holds in the nonlinear case [4], though adiabaticity breaks down if an eigenstate undergoes a bifurcation [5, 6].

We will focus on the one-dimensional case, which arises, for example, in confined geometries (see, e.g., [7] and references therein). Then the effective interaction strength is given by $g = 2\hbar^2 aN/Ma_\perp^2$, where a is the s-wave scattering length, $a_\perp$ is the transverse extension of the condensate and N is the number of atoms [8] and the wavefunction is normalized as $\|\psi\|^2 = 1$. The one-dimensional approximation is valid if the nonlinear interaction is not too strong. Stronger interactions will couple the axial and radial degrees of freedom. In this regime the non-polynomial Schrödinger equation provides a better description of the dynamics of a BEC [9].

For convenience we rescale the NLSE (2) such that $\hbar = M = 1$. This yields the NLSE in the convenient form

$$\frac{\mathrm{d}^2\psi}{\mathrm{d}x^2} = -q^2(x)\psi(x) + 2g|\psi(x)|^2\psi(x) \tag{3}$$

with $q^2(x) = 2(\mu - V(x))$. For the most important case of a harmonic trap $V(x) = m\omega^2 x^2/2$ discussed in section 4 this is achieved by rescaling the variables as

$$x' = x/\ell, \qquad \psi' = \sqrt{\ell}\psi, \qquad g' = \ell M g/\hbar^2 \qquad \text{and} \quad \mu' = \mu/(\hbar\omega) \tag{4}$$

with the standard length $\ell = \sqrt{\hbar/M\omega}$. The rescaled potential is $V(x) = x^2/2$ and the chemical potential is given in units of $\hbar\omega$. To get a feeling for the relevant dimensions consider a BEC of 10^4 atoms with transverse width $a_\perp = 10\ \mu$m. This yields a scaled nonlinearity of $g = +20$ for a ^{87}Rb BEC in a trap with axial frequency $\omega = 2\pi \times 2$ Hz and $g = -20$ for a ^{7}Li-BEC in a trap with $\omega = 2\pi \times 100$ Hz.

During the last decade a lot of work has been devoted to numerical solutions of the time-independent NLSE and the development of algorithms (see, e.g., [10] for harmonic traps and [11] for open system). Analytic solutions, however, are available only for some special cases, among these the free NLSE [12, 13], arrangements of delta potentials [14–16] and potentials given by Jacobi elliptic functions [17]. Thus there is a great interest in feasible approximations to the NLSE, among which the most popular one is the Thomas–Fermi approximation for the ground state in a trapping potential. An extension of the Thomas–Fermi approximation was discussed in [18], matching the approximate wavefunction in the classical allowed region to a smoothly vanishing wavefunction in the classical forbidden region. An iterative semiclassical method was used in [19] to calculate nonlinear scattering eigenfunctions. The nth-order approximation for the wavefunction, $\psi^{(n)}(x)$, is calculated using standard WKB methods with the potential $V(x) + g|\psi^{(n-1)}(x)|^2$, where the lowest order is given by the Thomas–Fermi approximation.

Recently two advanced semiclassical methods for the calculation of nonlinear eigenstates were proposed. In the common linear WKB theory, the 'action' is expanded with respect to the small parameter $\hbar$. This is generally not possible for the NLSE, as the interaction term introduces a new scale into the system. In a recent paper, Konotop and Kevrekidis identified $\delta \sim \hbar^2/g$ as a suitable small parameter for a nonlinear WKB approach [20]. The wavefunction $\psi(x)$ is expanded with respect to δ in an asymptotic series. In the vicinity of the classical turning points, the WKB solution is matched to a function with the correct asymptotics to avoid divergences.

Furthermore, a divergence-free WKB method avoiding the problems at the classical turning points was introduced recently [21, 22]. Here, one substitutes the ansatz $\psi(x) =$

$\exp(\varphi(x))$ into the linear Schrödinger equation. In contrast to the traditional WKB method, the kinetic term $\sim \mathrm{d}^2\varphi/\mathrm{d}x^2$ is eliminated by differentiating again with respect to x. This method can be generalized to construct the ground state wavefunction of the NLSE.

In the present paper, we discuss another semiclassical method to solve the time-independent NLSE approximately based on a mapping to Painlevé's second equation. Special attention will be paid to the shift of the chemical potential μ of bound states due to the nonlinear mean-field energy. This method provides good results for excited states and it is fairly easy to understand and to use.

Finally, let us note that the nonlinear Schrödinger equation also describes the propagation of electromagnetic waves in nonlinear media (see, e.g., [23], chapter 8).

2. The second Painlevé transcendent

One of the most famous ordinary differential equations with a cubic nonlinearity is Painlevé's second equation or, briefly, the P_{II} equation (see, e.g. [24, 25]),

$$\frac{\mathrm{d}^2\phi}{\mathrm{d}y^2} = 2\sigma\phi^3 + y\phi, \qquad \sigma = \pm 1. \tag{5}$$

The solutions $\phi_k(x)$, where the index k refers to the asymptotics at $y \to +\infty$, are transcendent. In the linear case, which is found for $\sigma = 0$, the P_{II} equation reduces to the Airy equation. In fact Airy functions are found in the asymptotic limit (see below).

In textbooks one mostly finds results for the repulsive case $\sigma = +1$. However, asymptotic expansions, which will prove itself as quite useful, are available for both cases [26, 27]. For $y \to +\infty$ the Painlevé transcendent $\phi_k(x)$ vanishes as

$$\phi_k(y) \sim k\mathrm{Ai}(y). \tag{6}$$

We can restrict ourselves to $k > 0$, since equation (5) is invariant under a sign change of $\phi(y)$. Connection formulae, which relate the asymptotic form for $y \to -\infty$ to the form for $y \to +\infty$, are well known [26, 27]. For $\sigma = +1$ and $k \geqslant 1$ the Painlevé transcendent diverges. Otherwise the solution is oscillatory for negative y with asymptotics

$$\phi_k(y) \sim d|y|^{-1/4} \sin\left(\tfrac{2}{3}|y|^{3/2} - \tfrac{3}{4}\sigma d^2 \ln|y| - \theta\right) + \mathcal{O}(|y|^{-7/4}). \tag{7}$$

The constants depend on the parameter k as

$$d^2(k) = -\frac{\sigma}{\pi}\ln(1 - \sigma k^2) \tag{8}$$

$$\theta(k) = \frac{3}{2}\sigma d^2(k)\ln 2 + \sigma \arg\left[\Gamma\left(1 - \frac{1}{2}\mathrm{i}d^2(k)\right)\right] - \frac{\pi}{4}. \tag{9}$$

The form of the second Painlevé transcendent is illustrated in figure 1. We plotted the Painlevé transcendent $\phi_k(y)$ in comparison with the asymptotic expansions (7) for $y < 0$ and (6) for $y > 0$ for $k = 0.5$ and $\sigma = \pm 1$. One observes that the asymptotic expansions are quite accurate already for small values of $|y|$.

Furthermore, note that the P_{II} equation with $\sigma = +1$ can be written as a Hamiltonian system [25]

$$\frac{\mathrm{d}\phi}{\mathrm{d}x} = \frac{\partial\mathcal{H}}{\partial p}, \qquad \frac{\mathrm{d}p}{\mathrm{d}x} = -\frac{\partial\mathcal{H}}{\partial\phi} \tag{10}$$

with the Hamiltonian function

$$\mathcal{H} = \frac{p^2}{2} - \left(\phi^2 + \frac{x}{2}\right)p - \frac{\phi}{2}. \tag{11}$$

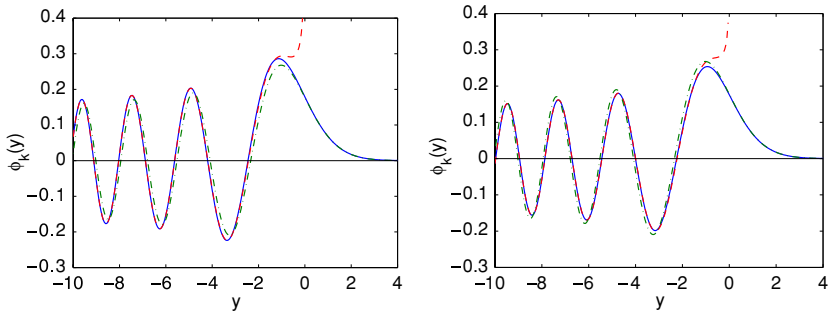

Figure 1. The Painlevé transcendent $\phi_k(y)$ (solid blue lines) for $k = 0.5$ and $\sigma = +1$ (left) and $\sigma = -1$ (right) in comparison with the asymptotic forms (7) (red dashed line) and $k\mathrm{Ai}(y)$ (green dash-dotted line).

3. The wedge potential

As a first illustrative example for the application of the P_{II} equation we consider the real-valued nonlinear eigenstates in a wedge potential

$$V(x) = F|x|. \tag{12}$$

This potential provides a natural and easily understandable example for the nonlinear quantization using the P_{II} transcendent. A gravitational wedge billiard for ultracold atoms has been realized by two blue-detuned laser beams which give rise to a repelling wedge-shaped dipole potential [28, 29]. At the boundary of a BEC, a linear approximation of the potential can be used for arbitrary traps [30]. Furthermore, the quantum states of cold neutrons in the earth's gravity potential above a hard wall corresponding to a half-wedge were measured recently [31].

We consider only real states with a defined parity $\psi(x) = (-1)^n\psi(-x)$, such that we can restrict our analysis to the positive real line, $x > 0$ and replace $|\psi(x)|^2\psi(x)$ by $\psi(x)^3$. By the means of a scaling $y = (2F)^{1/3}(x - \mu/F)$ and $\psi = |g|^{-1/2}(2F)^{1/3}\phi$, the NLSE with the wedge potential is transformed to the standard form

$$\frac{\mathrm{d}^2\phi}{\mathrm{d}y^2} = 2\sigma\phi^3 + y\phi \tag{13}$$

with $\sigma = \mathrm{sign}(g)$. The scaled variable y is negative in the classically allowed region $Fx < \mu$ such that the wavefunction is oscillatory. In the classically forbidden region $Fx > \mu$ one has $y > 0$ and the wavefunction vanishes as $\phi(y) \sim k\mathrm{Ai}(y)$. Note that the differential equation (13) does not depend on the nonlinear parameter g explicitly—this dependence is hidden in the normalization of $\phi_k(y)$. Rescaling the normalization condition $\|\psi\|^2 = 1$ yields

$$2\int_{y(x=0)}^{+\infty} |\phi_k(y)|^2\,\mathrm{d}y = \frac{|g|}{(2F)^{1/3}}. \tag{14}$$

The quantization condition can now be deduced from the asymptotic form (7) of the Painlevé transcendent. Note that the definition of a quantum number is not so straightforward as in the linear case, as new nonlinear eigenstates can emerge and disappear if the nonlinearity g is changed (see, e.g. [32]). However, if we restrict ourselves to the nonlinear eigenstates with a linear counterpart and thus a defined parity, the quantum number can be identified with the number of zeros of the wavefunction. Thus the relevant quantization condition is that the

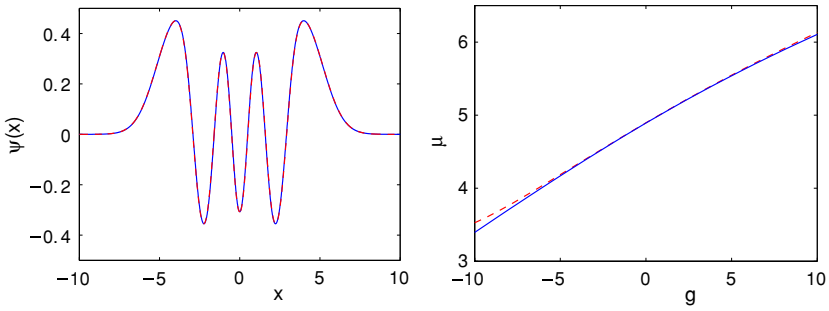

Figure 2. Nonlinear eigenstate with quantum number $n = 6$ of the NLSE for a wedge potential $V(x) = |x|$. Left: wavefunction for $g = 5$, right: dependence of the chemical potential on the nonlinearities g. The semiclassical results (dashed red line) are compared to numerically exact results (solid blue line).

wavefunction $\psi_n(x)$ must have n zeros. Due to the (anti)symmetry $\psi(x) = (-1)^n\psi(-x)$, the wavefunction assumes an extremum (n even) or a zero (n odd) at $x = 0$.

Using the asymptotic form (7) of the Painlevé transcendent, this condition can now be cast into an explicit form. As the asymptotic form of the P_{II} transcendent is basically given by a sine function, a condition for the argument of this sine function directly follows from the conditions on the wavefunction. In fact, the argument of the sine at $y\,(x = 0) = -2^{1/3}\mu/F^{2/3}$ must equal $(n + 1)\pi/2$. Inserting this into equation (7) yields the relevant quantization condition

$$\frac{(2\mu)^{3/2}}{3F} - \frac{3}{4}\sigma d^2(k_n)\ln\left(\frac{2^{1/3}\mu}{F^{2/3}}\right) - \theta(k_n) = \frac{n+1}{2}\pi, \tag{15}$$

where $d(k_n)$ and $\theta(k_n)$ are given by equations (8) and (9), respectively. The advantage of this method is that the problem of solving a nonlinear boundary value problem is reduced to a single algebraic equation.

However, calculating a nonlinear eigenstate with quantum number n for a given value of the nonlinear parameter g is not so easy. In fact one has to determine the chemical potential μ so that the quantization condition (15) and the normalization condition (14) are fulfilled *simultaneously*. This can be achieved by an iterative method. It is much easier, however, to start from a *fixed* value of μ. The quantization condition (15) then yields solutions k_n for different quantum numbers n. Given these values of k_n, one can calculate the Painlevé functions $\phi_k(y)$ and the effective nonlinear parameter $g_n(\mu)$ from the normalization integral (14). Rescaling the variables to x and ψ again directly gives the wavefunction $\psi(x)$. Such renormalization procedures are also inevitable in many numerical schemes for the computation of nonlinear eigenstates (cf [11]).

To test the feasibility of this approach, we consider the nonlinear eigenstate $n = 6$ for a wedge potential with $F = 1$. The resulting wavefunction is shown in figure 2 on the left-hand side (dashed red line) in comparison with the numerically exact solution (solid blue line). Both wavefunctions are indistinguishable on the scale of drawing. The right side shows the dependence of the chemical potential on the nonlinearity g, again in comparison to the numerically exact values. One observes a good agreement. The numerical results for the NLSE solutions were obtained using the standard boundary-value solver `bvp4c` of MATLAB.

Let us again note that the nonlinear eigenstates analysed in this section are no eigenstates in the sense of linear algebra. In particular there is no superposition principle and the dynamics of an arbitrary wavepacket cannot be decomposed into eigenstates. However, the nonlinear

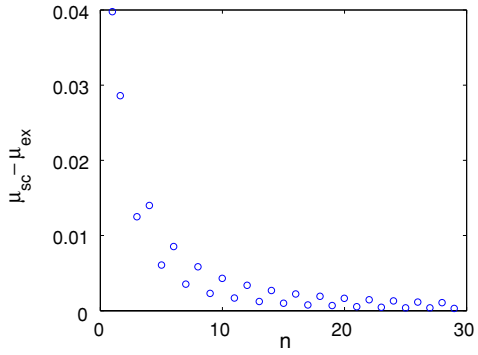

Figure 3. Solution of the NLSE for a wedge potential: error of the semiclassical calculation of the chemical potential $\mu_{\mathrm{sc}} - \mu_{\mathrm{ex}}$ in dependence of the quantum number n for $g = 5$.

eigenstates are still stationary states of the time-dependent NLSE. Small perturbation will not affect the dynamics seriously unless the eigenstates undergo a bifurcation as predicted by the nonlinear adiabatic theorem [4]. The phase of the states varies as $\exp(-\mathrm{i}\mu t)$, where the shift of the chemical potential μ with the nonlinearity g is conveniently described by the semiclassical model.

The only error in this calculation results from the replacement of the P_{II} transcendent by its asymptotic form (7). This error vanishes rapidly for larger quantum numbers n, which is illustrated in figure 3. The extrema of the P_{II} transcendent are given less accurately by the asymptotic form than the zeros. Thus the error is larger for even quantum number n.

4. The harmonic potential

Now we want to extend the quantization method presented in the previous section to a more important application—the harmonic trap

$$V(x) = \frac{x^2}{2}. \tag{16}$$

A common method used in semiclassics is a comparison of the Schrödinger equation to a well-known differential equation, such as Airy's equation [33, 34]. Similarly we will map the NLSE for the harmonic trap to the P_{II} equation.

We use the mapping ansatz

$$\psi(x) = af(x)\phi(y(x)), \tag{17}$$

well known for the linear Schrödinger equation [34], however with an additional scaling constant a. Differentiating twice gives

$$\frac{1}{a}\frac{\mathrm{d}^2\psi}{\mathrm{d}x^2} = \frac{\mathrm{d}^2 f}{\mathrm{d}x^2}\phi + 2\frac{\mathrm{d}f}{\mathrm{d}x}\frac{\mathrm{d}\phi}{\mathrm{d}y}\frac{\mathrm{d}y}{\mathrm{d}x} + f\frac{\mathrm{d}\phi}{\mathrm{d}y}\frac{\mathrm{d}^2 y}{\mathrm{d}x^2} + f\left(\frac{\mathrm{d}y}{\mathrm{d}x}\right)^2\frac{\mathrm{d}^2\phi}{\mathrm{d}y^2}. \tag{18}$$

We demand that the terms proportional to $\mathrm{d}\phi/\mathrm{d}y$ cancel, which leads to the condition

$$2\frac{\mathrm{d}f}{\mathrm{d}x}\frac{\mathrm{d}y}{\mathrm{d}x} + f\frac{\mathrm{d}^2 y}{\mathrm{d}x^2} = 0 \quad \Rightarrow \quad f(x) = \left(\frac{\mathrm{d}y}{\mathrm{d}x}\right)^{-1/2}. \tag{19}$$

Furthermore the term proportional to $\mathrm{d}^2 f/\mathrm{d}x^2$ is assumed to be small and can be neglected. Substituting the P_{II} equation (5) and the NLSE (3) into equation (18) finally yields

$$\left(\frac{\mathrm{d}y}{\mathrm{d}x}\right)^2 [2\sigma\phi^3 + y\phi] + q^2(x)\phi - 2ga^2\left(\frac{\mathrm{d}y}{\mathrm{d}x}\right)^{-1}\phi^3 = 0. \tag{20}$$

In the linear world, which is given by $g = 0$ or $\sigma = 0$ respectively, this directly gives a differential equation that determines the mapping $y(x)$. If the nonlinear effects are small, we can neglect the nonlinear terms in the mapping equation which yields

$$\left(\frac{\mathrm{d}y}{\mathrm{d}x}\right)^2 = \frac{-q^2(x)}{y(x)}. \tag{21}$$

The scaling constant a is now chosen such that the error due to the neglect of the nonlinear terms in the mapping equation (21) is as small as possible. In the fashion of a least-squares fit, a is chosen such that the error

$$\chi^2 = \int_{-\infty}^{\infty}\left[\sigma\left(\frac{\mathrm{d}y}{\mathrm{d}x}\right)^2 - ga^2\left(\frac{\mathrm{d}y}{\mathrm{d}x}\right)^{-1}\right]^2 \phi(y(x))^6\,\mathrm{d}x \tag{22}$$

is minimal. This can be done at the end of the calculation, after $\phi(y(x))$ has been determined.

This mapping can now be used to approximately calculate eigenstates in symmetric single minimum potentials at $x = 0$, e.g. a harmonic trap $V(x) = x^2/2$. For wavefunctions with a linear counterpart, that have a defined parity, we can restrict our analysis to $x \geqslant 0$. To avoid a divergence at the classical turning point x_t the mapping has to be such that $y(x_t) = 0$. Thus the integrating equation (21) yields the mapping in explicit form

$$y(x) = \pm\left[\pm\frac{3}{2}\int_{x_t}^{x}\sqrt{|q^2(x')|}\,\mathrm{d}x'\right]^{2/3}, \tag{23}$$

where the $-$ sign is taken in the classically allowed region $x < x_t$ and the + sign is taken in the classically forbidden region $x > x_t$.

The quantization condition is deduced from the asymptotic form of the Painlevé transcendent (7) exactly as in section 3. The only difference is that the mapping is now given by equation (23), such that the expression for $y\,(x = 0)$ is a little more complicated. Thus the relevant quantization condition is given by

$$\frac{2}{3}|y(0)|^{3/2} - \frac{3}{4}\sigma d^2(k_n)\ln|y(0)| - \theta(k_n) = \frac{n+1}{2}\pi. \tag{24}$$

To test the feasibility of this approach, we consider the nonlinear eigenstates for a harmonic potential $V(x) = x^2/2$. The result for the eigenfunctions with $n = 10$ is shown in figure 4. The left-hand side shows the wavefunction calculated using the mapping procedure (dashed red line) in comparison with the numerically exact solution (solid blue line). The right-hand side shows the dependence of the chemical potential on the nonlinearity g, again in comparison to the numerically exact values. One observes a good agreement.

Figure 5 shows results for different quantum numbers n. The error of the semiclassical calculation, i.e. the difference of the semiclassical value for the chemical potential μ_{sc} and the numerically exact value μ_{ex}, is plotted against the quantum number n for $g = 1$ and $g = 10$. Except for very small values of n and $g = 10$, for which the reduction to the asymptotic form (7) is not valid, one obtains reasonable results for the semiclassical approximation.

The method introduced above can be extended to asymmetric trapping potentials. Then one has to construct solutions around the two classical turning points separately, which are matched at a 'mid-phase point' [33]. In this spirit the restriction to symmetric or anti-symmetric solutions above is nothing but a matching of two solutions at the mid-phase point $x = 0$.

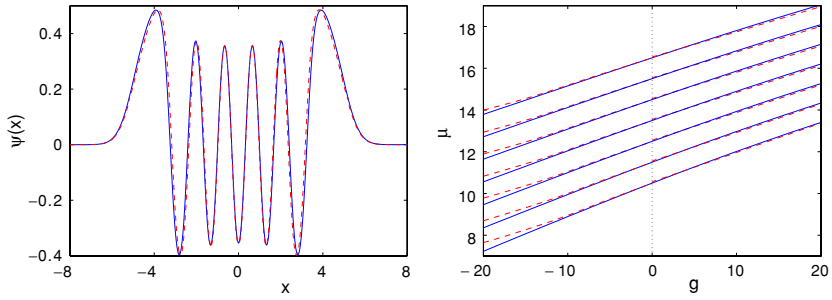

Figure 4. Nonlinear eigenstates of the NLSE in a harmonic potential $V(x) = x^2/2$. Left: wavefunction of the eigenstate with quantum number $n = 10$ for $g = 10$, right: dependence of the chemical potential on the nonlinearities g for the eigenstates $n = 10 - 16$. The semiclassical results (dashed red line) are compared to numerically exact results (solid blue line).

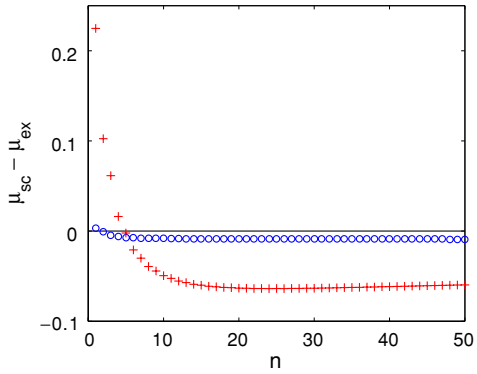

Figure 5. Solution of the NLSE for a harmonic potential: error of the semiclassical calculation of the chemical potential $\mu_{\rm sc} - \mu_{\rm ex}$ in dependence of the quantum number n for $g = 1$ (blue circles) and $g = 10$ (red crosses).

In the linear case $g = 0$, a mapping to a similar potential with two classical turning points, in fact the harmonic potential, avoids this matching procedure [34]. In the nonlinear case, however, the single-turning point equation P_{II} has some advantages compared to the NLSE with a harmonic potential because the P_{II} equation is free of movable branch points and connection formulae are well known.

5. Mapping to a constant potential

The mapping technique introduced above can easily be generalized to other setups. In this section we demonstrate the calculation of nonlinear eigenstates in a weak periodic potential by a mapping to the free NLSE. It is well known that the free NLSE

$$\frac{\mathrm{d}^2\phi}{\mathrm{d}y^2} + 2\nu\phi(y) - 2g\phi(y)^3 = 0 \tag{25}$$

has soliton solutions. Bright solitons are found for $\nu < 0$ and $g < 0$, given by

$$\phi(y) = \sqrt{2\nu/g}\,\mathrm{sech}\,(\sqrt{-2\nu}(y - y_0)), \tag{26}$$

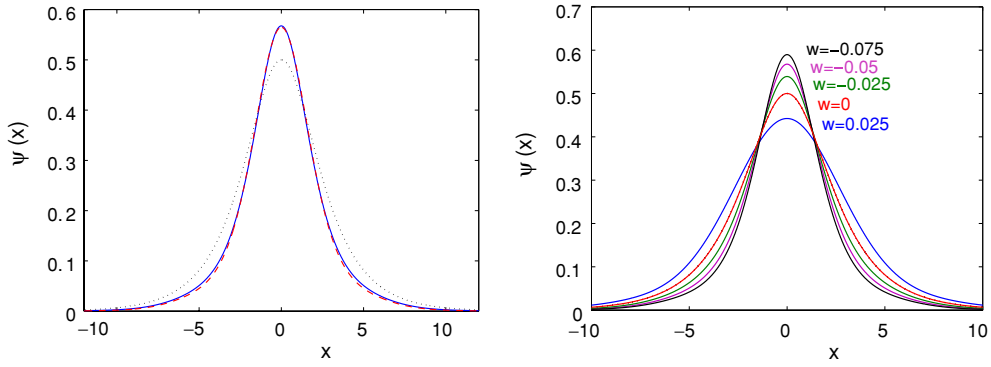

Figure 6. Left: bright soliton solution in a cosine potential of strength $w = -0.05$ for $g_{\mathrm{eff}} = -1$. Numerically exact results (solid blue line) are compared to results from the mapping technique (dashed red line). The bright soliton solution for $w = 0$ (26) is also plotted as a reference (black dotted line). Right: bright soliton solution for $g_{\mathrm{eff}} = -1$ and different values of w.

and dark solitons for $\nu > 0$ and $g > 0$ are given by

$$\phi(y) = \sqrt{\nu/g}\,\tanh\left(\sqrt{\nu}(y - y_0)\right). \tag{27}$$

Using a mapping technique as in the previous section we explore the effects of a small additional cosine potential on these solitons. In fact we consider the NLSE

$$\frac{\mathrm{d}^2\psi}{\mathrm{d}x^2} + 2(\mu - w\cos(x))\psi(x) - 2g\psi(x)^3 = 0. \tag{28}$$

Using again the ansatz (17) and following the lines of reasoning of section 4, one arrives at

$$\left(\frac{\mathrm{d}y}{\mathrm{d}x}\right)^2 [2g\phi^3 - 2\nu\phi] + 2(\mu - v\cos(x))\phi - 2ga^2\left(\frac{\mathrm{d}y}{\mathrm{d}x}\right)^{-1}\phi^3 = 0. \tag{29}$$

Again one chooses the scaling factor a to minimize the difference of the nonlinear terms

$$\chi^2 = \int_{-\infty}^{\infty}\left[g\left(\frac{\mathrm{d}y}{\mathrm{d}x}\right)^2 - ga^2\left(\frac{\mathrm{d}y}{\mathrm{d}x}\right)^{-1}\right]^2 \phi(y(x))^6\,\mathrm{d}x \tag{30}$$

and neglects them in equation (29) to arrive at the mapping equation

$$\left(\frac{\mathrm{d}y}{\mathrm{d}x}\right)^2 = \frac{\mu - w\cos(x)}{\nu}. \tag{31}$$

To ensure that the right-hand side is positive, one must always be in the classically allowed region ($\mu > w$, thus $\nu > 0$) or the classically forbidden region ($\mu < -w$, thus $\nu < 0$); values in the interval $\mu \in (-w, w)$ cannot be treated within this framework.

To show the validity of this method, we calculate a bright soliton solution in a cosine lattice $V(x) = w\cos(x)$. The left-hand side of figure 6 shows the wavefunction calculated by the mapping method in comparison to the numerically exact solution. One observes a good agreement. A systematic deformation of the wavefunction in comparison to the free soliton is observed, which is well described by the mapping procedure. This is further illustrated on the right-hand side of figure 6, where the soliton wavefunction is plotted for different values of the potential strength w. The deformation of the soliton can be understood as a perturbative effect. For $w < 0$, a potential minimum is created around $x = 0$ attracting the condensate and thus

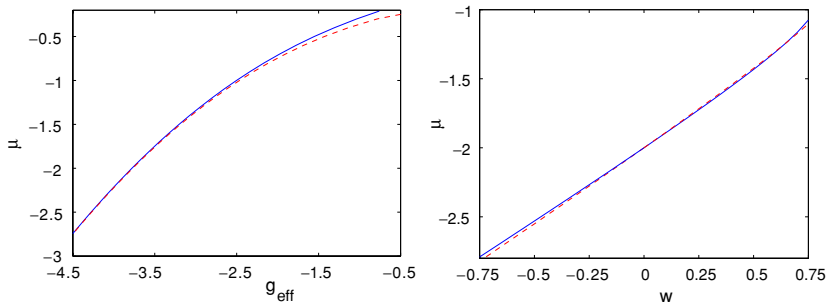

Figure 7. Shift of the chemical potential of a bright soliton in a cosine potential in dependence of the nonlinearity g_{eff} for $w = -0.2$ (left) and in dependence of the potential strength w for $g_{\mathrm{eff}} - 4$ (right). Numerically exact results (solid blue line) are compared to results from the mapping technique (dashed red line).

increasing the intensity at this position. Altogether the soliton is narrowed. Correspondingly a potential maximum at $x = 0$ repels the condensate and the soliton becomes broader for $w > 0$. In terms of the mapping solution, the deformation of the soliton is described by the scaling function $f(x) = (\mathrm{d}y/\mathrm{d}x)^{-1/2}$. For $w < 0$ one has $f(0) > 1$ such that the height of the soliton increases. The height is reduced for $w > 0$, where $f(0) < 1$.

Furthermore we calculate the dependence of the chemical potential μ of such a bright soliton on the nonlinearity g_{eff} for a fixed value of w and on the potential strength w for a fixed nonlinearity g_{eff}. The results obtained by the mapping method and the numerically exact results are compared in figure 7. One observes a good agreement.

Concluding this section, we have shown that a bright soliton solution survives in the presence of a weak perturbative potential. The effects of this perturbation can be described by a mapping technique. The soliton is narrowed or broadened depending on whether it is situated in a potential well or at a potential maximum. Consequently its chemical potential is decreased or increased.

Acknowledgments

Support from the Studienstiftung des deutschen Volkes and the Deutsche Forschungsgemeinschaft via the Graduiertenkolleg ‘Nichtlineare Optik und Ultrakurzzeitphysik’ is gratefully acknowledged. We thank R S Kaushal for stimulating discussions and the anonymous referee for a very valuable and careful report, helping us to improve the final version of the manuscript.

References

[1] Pitaevskii L and Stringari S 2003 *Bose–Einstein Condensation* (Oxford: Oxford University Press)
[2] Smerzi A, Fantoni S, Giovanazzi S and Shenoy S R 1997 *Phys. Rev. Lett.* **79** 4950
[3] Albiez M, Gati R, Fölling J, Hunsmann S, Cristiani M and Oberthaler M K 2005 *Phys. Rev. Lett.* **95** 010402
[4] Liu J, Wu B and Niu Q 2003 *Phys. Rev. Lett.* **90** 170404
[5] Wu B and Niu Q 2000 *Phys. Rev.* A **61** 023402
[6] Witthaut D, Graefe E M and Korsch H J 2006 *Phys. Rev.* A **73** 063609
[7] Greiner M, Bloch I, Mandel O, Hänsch T W and Esslinger T 2001 *Appl. Phys.* B **73** 769
[8] Olshanii M 1998 *Phys. Rev. Lett.* **81** 938
[9] Salasnich L, Parola A and Reatto L 2002 *Phys. Rev.* A **65** 043614
[10] Dalfovo F and Stringari S 1996 *Phys. Rev.* A **53** 2477

[11] Schlagheck P and Paul T 2006 *Phys. Rev.* A **73** 023619
[12] Carr L D, Clark C W and Reinhardt W P 2000 *Phys. Rev.* A **62** 063610
[13] Carr L D, Clark C W and Reinhardt W P 2000 *Phys. Rev.* A **62** 063611
[14] Witthaut D, Mossmann S and Korsch H J 2005 *J. Phys. A: Math. Gen.* **38** 1777
[15] Witthaut D, Rapedius K and Korsch H J 2005 *Preprint* cond-mat/0506645
[16] Seaman B T, Carr L D and Holland M J 2005 *Phys. Rev.* A **71** 033622
[17] Bronski J C, Carr L D, Deconinck B and Kutz J N 2001 *Phys. Rev. Lett.* **86** 1402
[18] Band Y B, Towers I and Malomed B A 2003 *Phys. Rev.* A **67** 023602
[19] Paul T, Leboeuf P, Pavloff N, Richter K and Schlagheck P 2005 *Phys. Rev.* A **72** 063621
[20] Konotop V V and Kevrekidis P G 2003 *Phys. Rev. Lett.* **91** 230402
[21] Hyouguchi T, Adachi S and Ueda M 2002 *Phys. Rev. Lett.* **88** 170404
[22] Hyouguchi T, Seto R, Ueda M and Adachi S 2004 *Ann. Phys., NY* **312** 177
[23] Dodd R K, Eilbeck J C, Gibbon J D and Morris H C 1982 *Solitons and Nonlinear Wave Equations* (London: Academic)
[24] Iwasaki K, Kimura H, Shimomura S and Yoshida M 1991 *From Gauss to Painlevé: A Modern Theory of Special Functions* (Braunschweig: Vieweg)
[25] Ablowitz M J and Clarkson P A 1991 *Solitons, Nonlinear Evolution Equations and Inverse Scattering* (Cambridge: Cambridge University Press)
[26] Ablowitz M J and Segur H 1977 *Phys. Rev. Lett.* **38** 1103
[27] Segur H and Ablowitz M J 1981 *Physica* D **3** 165
[28] Milner V, Hanssen J L, Campbell W C and Raizen M G 2001 *Phys. Rev. Lett.* **86** 1514
[29] Andersen M F, Grünzweig T, Kaplan A and Davidson N 2004 *Phys. Rev.* A **69** 063413
[30] Dalfovo F, Pitaevskii L and Stringari S 1996 *Phys. Rev.* A **54** 4213
[31] Nesvizhevsky V V *et al* 2002 *Nature* **415** 297
[32] D'Agosta R and Presilla C 2002 *Phys. Rev.* A **65** 043609
[33] Miller H H 1968 *J. Chem. Phys.* **48** 464
[34] Berry M V and Mount K E 1972 *Rep. Prog. Phys.* **35** 315